

Exciton localization in AlGaN alloys

N. Nepal, J. Li, M. L. Nakarmi, J. Y. Lin, and H. X. Jiang^{a)}

Department of Physics, Kansas State University, Manhattan, Kansas 66506-2601

(Received 7 July 2005; accepted 21 December 2005; published online 6 February 2006)

Deep ultraviolet (UV) photoluminescence emission spectroscopy has been employed to study the exciton localization effect in AlGaN alloys. The temperature dependence of the exciton emission peak energy in $\text{Al}_x\text{Ga}_{1-x}\text{N}$ alloys ($0 \leq x \leq 1$) was measured from 10 to 800 K and fitted by the Varshni equation. Deviations of the measured data from the Varshni equation at low temperatures directly provide the exciton localization energies, E_{Loc} . It was found that E_{Loc} increases with x for $x \leq 0.7$, and decreases with x for $x \geq 0.8$. Our experimental results revealed that for AlGaN alloys, E_{Loc} obtained by the above method has simple linear relations with the localized exciton thermal activation energy and the emission linewidth, thereby established three parallel methods for directly measuring the exciton localization energies in AlGaN alloys. The consequence of strong carrier and exciton localization in AlGaN alloys on the applications of nitride deep UV optoelectronic devices is also discussed. © 2006 American Institute of Physics. [DOI: 10.1063/1.2172728]

AlGaN alloys have the capability of tuning the direct band gap in large energy range, from around 3.4 to 6.1 eV, which makes them very useful for ultraviolet (UV) and deep UV optoelectronic device applications. For device applications, high-quality AlGaN alloys are essential. It is therefore important to understand better structural, electronic, and optical properties of these alloys. One of the important properties, which affects the optical and electrical properties of AlGaN alloy, is the carrier and exciton localization. Exciton localization energy and photoluminescence (PL) emission linewidth yield the information about the compositional and potential fluctuations occurring in semiconductor alloys.

Theoretical and experimental investigations have been carried out to obtain a better understanding of the excitonic emission linewidth in semiconductor alloys.^{1–4} Coli *et al.* found that the emission linewidth of the excitonic transition in $\text{Al}_x\text{Ga}_{1-x}\text{N}$ alloys increases with Al concentration and reaches a maximum at $x \sim 0.7$, which implies that the potential fluctuation caused by alloy disorder is also a maximum at that value of x in $\text{Al}_x\text{Ga}_{1-x}\text{N}$ alloys. Potential fluctuation causes localization of carriers and excitons at low temperatures. Increase in fluctuating potential barriers in $\text{Al}_x\text{Ga}_{1-x}\text{N}$ alloys with x has been reported for $x \leq 0.25$.⁵ Increase in exciton localization energy with x in $\text{Al}_x\text{Ga}_{1-x}\text{N}$ alloys grown on GaN template for $x \leq 0.76$ has been previously reported by fitting data with Bose–Einstein expression in the temperature range between 200 and 300 K.⁶ An increase in exciton localization energy (E_{Loc}) from 7 to 34 meV as x increased from 0.05 to 0.35 was also measured by fitting the exciton emission peak energy with the Varshni equation in the temperature range of $T \leq 300$ °K.⁷ However, the direct measurement of E_{Loc} from the Varshni equation and its relation with the localized exciton activation energy and low-temperature emission linewidth in the entire compositional range x , $0 \leq x \leq 1$, has not been previously established in $\text{Al}_x\text{Ga}_{1-x}\text{N}$ alloys.

In this work, the effect of exciton localization in $\text{Al}_x\text{Ga}_{1-x}\text{N}$ alloys was probed by deep UV PL emission spectroscopy. The exciton localization energy in $\text{Al}_x\text{Ga}_{1-x}\text{N}$ al-

loys of the entire composition range ($0 \leq x \leq 1$) has been measured by fitting the excitonic emission peak energy with the Varshni equation. The relations between the exciton localization energy, the activation energy, and the emission linewidth have been established.

The 1 μm thick $\text{Al}_x\text{Ga}_{1-x}\text{N}$ alloys were grown by metalorganic chemical vapor deposition on sapphire (0001) substrates. Trimethylgallium and trimethylaluminum were used as Ga and Al sources, respectively. Energy dispersive x-ray microanalysis and x-ray diffraction (XRD) were employed to verify the Al contents. Atomic force microscopy and scanning electron microscopy studies revealed excellent surface morphologies. Structural characterization was done with XRD measurement. The samples were mounted on a high-temperature stage with a cold finger in a closed-cycle helium refrigerator and temperature was controlled between 10 and 800 K. The deep UV PL spectroscopy system consists of a frequency quadrupled 100 femtosecond Ti: Sapphire laser with an average power of 3 mW and repetition rate of 76 MHz at 196 nm, and a 1.3 m monochromator with a detection capability ranging from 185–800 nm.⁸

The temperature evolutions of the PL spectra of $\text{Al}_x\text{Ga}_{1-x}\text{N}$ alloys have been measured between 10 and 800 K for the entire composition range. Figure 1 shows the temperature evolution of the PL spectra for one representative $\text{Al}_x\text{Ga}_{1-x}\text{N}$ sample with $x=0.5$. The dominant emission line at 10 K (4.61 eV) is attributed to the localized exciton transition.^{1–7} The PL emission intensity, I_{emi} , decreases with increasing temperature due to thermal activation of the localized excitons. The spectral peak position is redshifted from 4.61 eV at 10 K to 4.25 eV at 800 K due to the variation of the band gap with temperature. The energy band-gap variation with temperature for different semiconductors has been previously studied by fitting with different equations.^{6,7,9–13} Among them the Varshni equation is the most common to study the nonlinear temperature dependence of the band gap. Figure 2 shows the temperature dependence of the exciton emission peak energy measured between 10 and 600 K for different x ($0 \leq x \leq 1$). The solid lines are the least-squares fit of the experimental results with the Varshni equation for $T > 200$ K for $\text{Al}_x\text{Ga}_{1-x}\text{N}$ alloys,

^{a)}Electronic mail: jiang@phys.ksu.edu

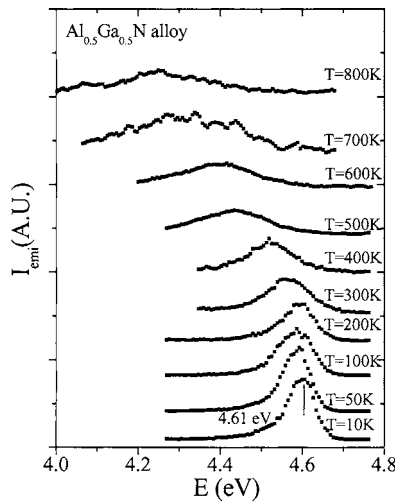


FIG. 1. PL spectra of Al_{0.5}Ga_{0.5}N alloy measured from 10 to 800 K.

$$E_g(T, x) = E_g(0, x) - \frac{\alpha(x)T^2}{\beta(x) + T}, \quad (1)$$

where $E_g(0, x)$ is the band gap of Al_xGa_{1-x}N alloy at $T = 0$ K; $\alpha(x)$ is an empirical constant; and $\beta(x)$ is associated with the Debye temperature.

At low temperatures, the exciton localization dominates and the PL emission peak energy is lower than the energy value predicted by Eq. (1) by an amount of the localization energy. At higher temperatures, the PL emission peak follows the temperature dependence described by Eq. (1). Thus, the deviation at the lowest measurement temperature provides a direct measure of the exciton localization energy. Figure 3(a) plots E_{Loc} as a function of x for Al_xGa_{1-x}N alloys, which clearly shows that the exciton localization energy, E_{Loc} , obtained by measuring the deviation from the Varshni equation at low-temperature increases with x and reaches maximum for $x=0.7$. The measured value of E_{Loc} in Al_{0.7}Ga_{0.3}N alloys is about 95 meV, which is the largest exciton localization energy ever reported for semiconductor alloys. In semiconductor alloys, the excitons are localized at low temperatures

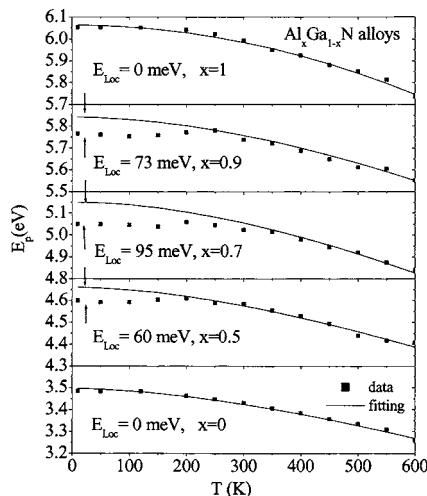


FIG. 2. The temperature dependence of the excitonic emission peak energy between 10 and 600 K for different x ($0 \leq x \leq 1$). The solid lines are the least-squares fit of the data with the Varshni equation, Eq. (1). Deviations from Eq. (1) at the lowest measurement temperatures are the measures of the exciton localization energies, E_{Loc} .

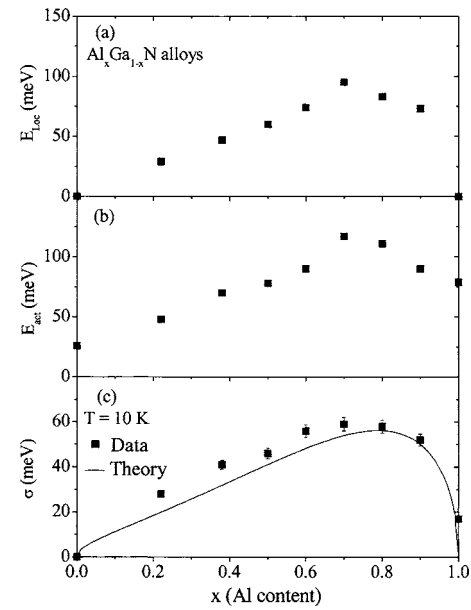


FIG. 3. Variations of the (a) exciton localization energy (E_{Loc}), (b) thermal activation energy (E_{act}), and (c) full width at half maximum (σ) of the PL emission line with Al content (x) in Al_xGa_{1-x}N alloys. E_{Loc} , E_{act} , and σ all increase with x for $x \leq 0.7$, decrease with x for $x \geq 0.8$, and have a maximum at $x \sim 0.7$. [The solid curve in (c) is a calculation result of Eq. (3)].

and free at higher temperatures. The onset temperature for the localized excitons to become free depends on the degree of localization. Due to the large values of the exciton localization energies, this onset temperature is much higher in Al_xGa_{1-x}N than in other semiconductor alloy systems and increases with x (for $x < 0.7$). Thus, a wide measurement temperature range is required in order to obtain E_{Loc} accurately.

The integrated emission intensity (I_{emi}) of the localized exciton transition between 150 and 400 K for samples with different x ($0 \leq x \leq 1$) can be well described by the thermal activation process

$$\ln(I_{emi}) = \ln(I_0) - \left(\frac{E_{act}}{k}\right) \frac{1}{T}, \quad (2)$$

where E_{act} is the activation energy, and k is the Boltzmann constant. The fitted values of E_{act} as a function of Al content, x are plotted in Fig. 3(b). Similar to the behavior of E_{Loc} shown in Fig. 3(a), the activation energy also increases with x for $x \leq 0.7$ and decreases with x for $x \geq 0.8$.

Alloy fluctuations also lead to a statistical distribution in the excitonic transition energies, which causes the emission linewidth broadening. The dependence of the full width at half maximum (σ) of the exciton emission line on composition, x , can be calculated by employing a quantum statistical approach assuming completely random alloys and is given by²⁻⁴

$$\sigma(x) = 0.41 \frac{dE_g(x)}{dx} \sqrt{8 \ln(2)x(1-x) \frac{V_c(x)}{4\pi a_{ex}^2(x)/3}}, \quad (3)$$

where $dE_g(x)/dx$ describes the variation of the direct band-gap energy with alloy composition, $V_c(x) = a_0^3(x)/\sqrt{2}$ is the volume of primitive cell, and $a_{ex} = \epsilon \hbar^2 / \mu e^2$ is the exciton Bohr radius. To calculate the value of $\sigma(x)$ in Al_xGa_{1-x}N alloys, we have used the physical values given in Refs. 3 and 4. We have used lattice constant in the hexagonal plane,

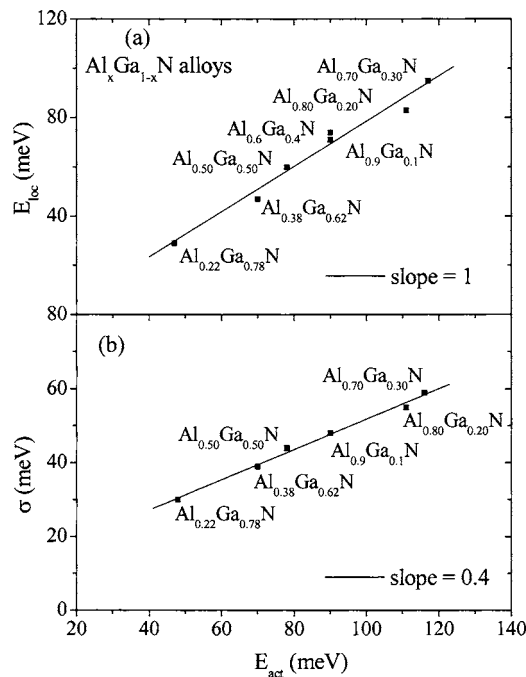


FIG. 4. (a) Exciton localization energy (E_{Loc}) as a function of the thermal activation energy (E_{act}) of the localized exciton in AlGaIn alloys. Solid line is a linear fit with a slope of 1. (b) Measured full width at half maximum (σ) of the localized exciton emission line as a function of E_{act} in AlGaIn alloys. Solid line is a linear fit with a slope of 0.4.

$a_0(x) = 3.160(1-x) + 3.112x$ (Å), dielectric constant $\epsilon(x) = 9.6(1-x) + 6.3x$, effective masses of electrons and holes $m_e/m_0 = 0.22(1-x) + 0.33x$ and $m_h = 1.5m_0$, where m_0 is the electron mass in the free space. The variation of the band-gap energy $E_g(x)$ is given as

$$E_g(x) = (1-x)E_g(\text{GaIn}) + xE_g(\text{AlIn}) - bx(1-x), \quad (4)$$

where b is the bowing parameter. We have used low-temperature ($T=10$ K) band gap $E_g(\text{GaIn})=3.5$ eV, $E_g(\text{AlIn})=6.1$ eV, and $b=1$ eV. The measured (squares) and calculated (solid curve) variations of $\sigma(x)$ with x for $0 \leq x \leq 1$ are shown in Fig. 3(c). The error bars for the experimental data are indicated for each x . In the experimental data, we have subtracted σ of GaN at 10 K to consider only the compositional disorder. Experimental results appear to be in good agreement with the theoretical calculation. The variation of σ with x follows the same trend as the localization energy and thermal activation energy shown in Figs. 3(a) and 3(b) and σ increases with x for $x \leq 0.7$ and decreases with x for $x \geq 0.8$. The alloy fluctuation (or σ) is a maximum at $x \sim 0.7$ instead at $x \sim 0.5$. This is because $\sigma(x)$ depending primarily on two terms, $\sigma(x) \propto \sqrt{x(1-x)} \cdot dE_g(x)/dx$. Although $\sqrt{x(1-x)}$ is symmetric and has a maximum around $x=0.5$, $dE_g(x)/dx$ increases linearly with x . This combination makes $\sigma(x)$ non-symmetric about $x \sim 0.5$ and having a maximum at $x \sim 0.7$ instead at $x \sim 0.5$.

To see the correlation between the localized exciton parameters, in Fig. 4(a), we plot the exciton localization energy obtained by measuring the peak energy deviations from the Varshni equation (E_{Loc}) at 10 K as a function of the thermal activation energy of the excitonic emission intensity (E_{act}).

The solid line is a linear fit of the experimental data with a slope of 1. This establishes the identical characteristic of E_{Loc} and E_{act} in $Al_xGa_{1-x}N$ alloys. In Fig. 4(b), we plot the variation of σ with E_{act} . The solid line is a linear fit of the experimental data with a slope of 0.4 indicating a linear correlation between the exciton localization energy and the emission linewidth in $Al_xGa_{1-x}N$ alloys. A linear relation, $\sigma=0.26 E_{Loc}$, between the localization energy and emission linewidth has been previously found in $ZnSe_xTe_{1-x}$ alloys.¹⁴

In summary, we have studied the exciton localization effect in $Al_xGa_{1-x}N$ alloys for the entire composition range, $0 \leq x \leq 1$. Our experimental results demonstrated that the localized excitons in AlGaIn alloys have the largest localization energies compared to all other semiconductor alloys. We have established effective methods for directly measuring the exciton localization energies (E_{Loc}) in AlGaIn alloys, and confirmed that E_{Loc} can be obtained by measuring either the deviation of the exciton emission peak energy with the Varshni equation at low temperatures or the thermal activation energy of the exciton emission intensity or the exciton emission linewidth. The exciton localization energy in $Al_xGa_{1-x}N$ alloys was observed to increase with x and reach maximum for $x \sim 0.7$, implying that the potential fluctuation caused by alloy disorder is also a maximum at that value of x , consistent with the theoretical calculation result assuming completely random alloys.^{3,4} Exciton localization is prominent in wide-gap AlGaIn alloys due to their small Bohr radius and a large difference in energy band gaps between GaIn and AlIn. This large exciton localization may give rise to increased quantum efficiency due to reduction of nonradiative recombination rate under the influence of the carrier localization effect. However, carrier localization will reduce significantly the conductivity of AlGaIn alloys, particularly for Al content around 70%. Thus, strong carrier and exciton localization can have a significant effect on the optical and electrical properties of deep UV optoelectronic devices.

This research is supported by the DOE (No. 96ER45604).

¹H. X. Jiang, L. Q. Zu, and J. Y. Lin, Phys. Rev. B **42**, 7284 (1990).

²M. S. Lee and K. K. Bajaj, J. Appl. Phys. **73**, 1788 (1993).

³G. Coli, K. K. Bajaj, J. Li, J. Y. Lin, and H. X. Jiang, Appl. Phys. Lett. **78**, 1829 (2001).

⁴G. Coli, K. K. Bajaj, J. Li, J. Y. Lin, and H. X. Jiang, Appl. Phys. Lett. **80**, 2907 (2002).

⁵A. Bell, S. Srinivasan, C. Plumlee, H. Omiya, F. A. Ponce, J. Christen, S. Tanaka, A. Fujioka, and Y. Nakagawa, J. Appl. Phys. **95**, 4670 (2004).

⁶B. K. Meyer, G. Steude, A. Goldner, A. Hofmann, H. Amano, and I. Akasaki, Phys. Status Solidi **216**, 187 (1999).

⁷H. S. Kim, R. A. Mair, J. Li, J. Y. Lin, and H. X. Jiang, Appl. Phys. Lett. **76**, 1252 (2000).

⁸(<http://www.phys.ksu.edu/area/GaNgroup>)

⁹K. P. O'Donnell and X. Chen, Appl. Phys. Lett. **58**, 2924 (1991).

¹⁰E. Grilli, M. Guzzi, R. Zamboni, and L. Pavesi, Phys. Rev. B **45**, 1638 (1992).

¹¹W. Bludau, A. Onton, and W. Heinke, J. Appl. Phys. **45**, 1846 (1974).

¹²Y. Li, Y. Lu, H. Chen, M. Wraback, M. G. Brown, M. Schurman, L. Koszi, and R. A. Stall, Appl. Phys. Lett. **70**, 2458 (1997).

¹³Y. P. Varshni, Physica (Amsterdam) **34**, 149 (1967).

¹⁴S. Lankes, H. Stanzl, K. Wolf, M. Giegler, and W. Gebhardt, J. Phys.: Condens. Matter **7**, 1287 (1995).